

# A Hybrid Dynamical Model for Hysteretic Thermal Shape Memory Alloy Wire Actuators<sup>\*</sup>

Michele A. Mandolino<sup>\*</sup> Francesco Ferrante<sup>\*\*</sup>  
Gianluca Rizzello<sup>\*</sup>

<sup>\*</sup> *Department of Systems Engineering, Department of Material Science and Engineering, 66123 Saarland University, Saarbrücken, (e-mail: {michele.mandolino, gianluca.rizzello}@imsl.uni-saarland.de)*

<sup>\*\*</sup> *Univ. Grenoble Alpes, CNRS, Grenoble INP, GIPSA-lab, 38000 Grenoble, France (e-mail: francesco.ferrante@univ-grenoble-alpes.fr)*

---

**Abstract:** In this paper, we present a novel hybrid dynamical model for hysteretic actuators consisting of spring-loaded Shape Memory Alloy (SMA) wires. The hybrid description is obtained by reformulating a set of physics-based ODEs resulting from the Müller-Achenbach-Seelecke (MAS) model of SMA material. Although the MAS model provides an accurate and consistent description of the system hysteresis, its use for simulation and control is limited due to the highly nonlinear and stiff nature of the resulting ODEs. By means of the hybrid reformulation, the numerical stiffness can be effectively eliminated while keeping all the benefits of the physics-based description. The different operating modes and transitions are first described from a physical point of view and then used to develop the flow and jump dynamics of the resulting hybrid model. Numerical simulations show that both hybrid and physics-based models provide nearly identical results. In addition, it is observed that the former requires simulation times that are up to two orders of magnitude smaller than the latter.

*Keywords:* Shape Memory Alloy, Hybrid Systems, Hysteresis, Actuator, Modeling

---

## 1. INTRODUCTION

Thermal Shape Memory Alloys (SMAs) are a class of smart materials that contract if exposed to a heat source. This phenomenon is caused by a thermally-induced change in the crystallographic structure of the material. If the heat source is removed, the initial shape can be recovered after the application of an external force (provided, e.g., by a spring load). When used as actuators, SMAs are commonly shaped as wires made of Nickel-Titanium alloys. This specific shape allows to effectively heat the material via the Joule heating produced by the application of an electric current. Their intrinsic characteristics such as large strain (up to 4-8%), high energy density, lightweight, and self-sensing capability make them ideal candidates for the design of new technologically competitive transducers (Lagoudas (2008)). Typical SMA applications range from industrial valves (Tiboni et al. (2011)) to bio-inspired robots (Cianchetti et al. (2014)), to mention a few.

Although SMAs have several advantages over conventional actuators, they exhibit a strongly nonlinear behavior characterized by a rate-, temperature-, and load-dependent hysteresis. Several models have been developed to describe the hysteretic characteristic of this particular material. Many of them are based on mathematical operators such as in Toledo et al. (2017) and Shakiba et al. (2019), and allow to model the system in a given operational con-

dition. In contrast, physics-based models appears highly attractive to describe SMA wires under different operating conditions (e.g., in terms of environmental temperature, loading force, and input rate), thus ensuring robustness for model-based controllers (Lagoudas (2008); Seelecke and Müller (2004)). On the other hand, the high level of detail of physical models results in an increase in complexity that makes numerical simulation and control of such systems highly involved. To address these issues, some authors have investigated the possibility of describing hysteresis in a hybrid dynamical setting (e.g., Janaideh et al. (2012)). In this way, analysis and control of hysteretic systems can be conducted in a systematic and robust way, based on the tools available from the hybrid framework (Goebel et al. (2012)). In particular, if a physics-based hysteresis model is used as a starting point for the development of a hybrid reformulation, all the benefits of the former can be combined with the numerical efficiency and robustness of the latter. While hybrid reformulation of magnetic (Ramirez-Laboreo et al. (2019)) and electrostatic (Shao et al. (2016)) hysteresis already exist in literature, no formal hybrid models have been presented for the thermo-mechanical hysteresis of SMAs, to the best of our knowledge.

In this paper, we propose a novel hybrid dynamical model for spring-loaded SMA wire actuators. The result is grounded on a physics-based SMA description proposed by Müller-Achenbach-Seelecke (MAS) (Seelecke and Müller (2004)). Such a model well describes the behavior of SMA hysteresis under different operating conditions, but it is

---

<sup>\*</sup> Research by Francesco Ferrante is funded in part by ANR via project HANDY, number ANR-18-CE40-0010.

highly nonlinear and numerically stiff. A reduced order hybrid reformulation is then proposed for the MAS model, formalized in terms of jump and flow dynamics. By means of numerical simulations, it is shown how the hybrid model provides the same accuracy of the MAS one while requiring a significantly smaller simulation time. The developed model represents the starting point for future applications of hybrid control techniques to SMA systems.

The remainder of this paper is organized as follows. In Section 2, a SMA-spring actuator is described and its physical model is defined. Section 3 presents the development of the novel hybrid model, while comparative simulation studies are reported in Section 4. Finally, concluding remarks and future developments are discussed in Section 5.

### 1.1 Preliminaries on Hybrid Systems

We consider hybrid systems with state  $x \in \mathbb{R}^n$  of the form

$$\begin{cases} \dot{x} = f(x) & x \in C \\ x^+ \in G(x) & x \in D \end{cases} \quad (1)$$

where  $f: \mathbb{R}^n \rightarrow \mathbb{R}^n$  is the flow map,  $C \subset \mathbb{R}^n$  is the flow set,  $D \subset \mathbb{R}^n$  is the jump set, and  $G: \mathbb{R}^n \rightarrow \mathbb{R}^n$  the set-valued jump map. The above hybrid system shorthand notation is  $\mathcal{H} = (C, f, D, G)$ . A solution to  $\mathcal{H}$  is any hybrid arc defined over a subset of  $\mathbb{R}_{\geq 0} \times \mathbb{N}_0$  that satisfies the dynamics of  $\mathcal{H}$ . This solution is said *complete* if its domain is unbounded and *maximal* if it is not the truncation of another solution. We say that  $\mathcal{H}$  satisfies the *hybrid basic conditions* if:  $C$  and  $D$  are closed in  $\mathbb{R}^n$ ;  $f$  is continuous on  $C$ ,  $G$  is nonempty, outer semicontinuous, and locally bounded on  $D$ . Given a set  $S$ , we denote  $\mathcal{S}_{\mathcal{H}}(S)$  the set of all *maximal solutions*  $\phi$  to  $\mathcal{H}$  with  $\phi(0, 0) \in S$ . For more details on hybrid systems, see Goebel et al. (2012).

## 2. SMA-SPRING ACTUATOR

In this section, we first summarize the operating principle of the investigated SMA-spring actuator. Then, a control-oriented, physics-based model is developed to describe how the SMA wire strain (output) is affected by the electrical power applied to the wire (control input), as well as the environmental temperature (disturbance input). For further details regarding on the SMA wire model, see Seelecke and Müller (2004).

### 2.1 Actuator Description

A schematic representation of the investigated actuator system is shown in Fig. 1. It consists of a SMA wire mechanically connected to a linear spring. Both SMA and spring have one fixed end-point and one movable end-point. Additionally, the free ends of both elements are joined together into a common point, which is denoted as  $P$ . We define  $d$  as the constant distance between the fixed end-points of the SMA and the spring. If  $d$  is greater than the sum of the wire and spring initial lengths, a pre-tension is induced in the SMA. When heated with an electric current, the SMA contracts and thus point  $P$  moves to the right along the wire axis (Fig. 1(b)). When the input current is removed, the bias spring pulls back the SMA to its original configuration (Fig. 1(a)).

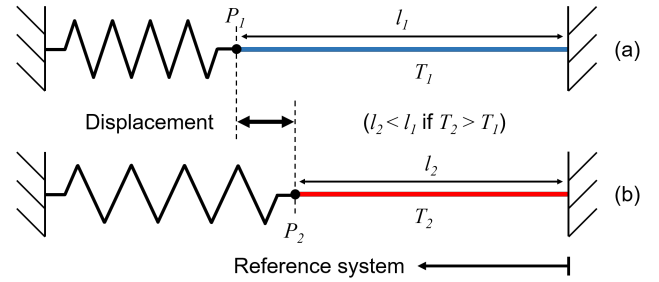


Fig. 1. Operating states of the actuator: SMA wire at the environmental temperature (a) and when heated (b).

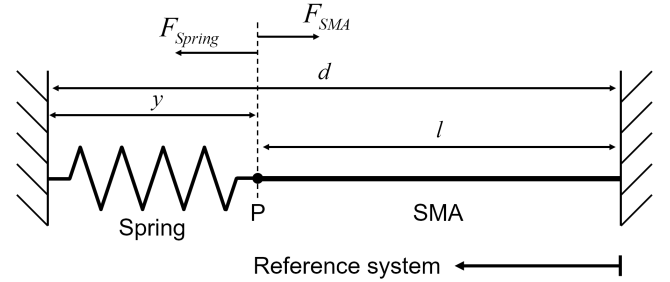


Fig. 2. Force diagram of the SMA-spring actuator.

### 2.2 SMA-spring physics-based model

A physics-based model of the SMA-spring actuator is developed in this section. We assume that the mass of the moving element is small, so that its inertial and gravitational effects are negligible compared to the thermo-elastic dynamics of the SMA. By considering the force diagram in Fig. 2, it is possible to obtain the force balance equation along the axis of the actuator

$$F_{Spring} - F_{SMA} = 0, \quad (2)$$

where  $F_{Spring}$  is the linear spring force, and  $F_{SMA}$  is the SMA force. Spring and SMA forces are given by

$$F_{Spring} = k(y - y_i), \quad (3)$$

$$F_{SMA} = \pi r_0^2 \sigma, \quad (4)$$

where  $k$  is the spring constant,  $y$  is the spring current length,  $y_i$  is the undeformed spring length, while  $r_0$  is the cross-sectional radius of the SMA wire, and  $\sigma$  is the stress that the SMA produces. It is possible to relate  $y$  to the total actuator length  $d$  as follows

$$y = d - l, \quad (5)$$

where  $l$  is the current length of the wire. The SMA length can be rewritten as

$$l = l_0(1 + \varepsilon), \quad (6)$$

where  $l_0$  is the length in undeformed and fully austenitic phase, and  $\varepsilon$  is the material strain. By replacing equations (3)-(6) in (2), we obtain

$$\pi r_0^2 \sigma + k(l_0 \varepsilon + l_0 + y_i - d) = 0. \quad (7)$$

As a next step, we need to characterize the stress in (7) by means of a material model. According to MAS, the stress-strain relationship of the material can be expressed as follows

$$\sigma = \sigma(\varepsilon, x_M, x_A) = \frac{\varepsilon - \varepsilon_T x_M}{\frac{x_M}{E_M} + \frac{x_A}{E_A}}, \quad (8)$$

where  $\varepsilon_T$  is the transformation strain,  $E_A$  and  $E_M$  are the austenite and martensite Young's moduli, while  $x_A$  and  $x_M$  are the austenite and martensite phase fractions, respectively. The phase fractions describe the relative amount of mesoscopic layers with the corresponding lattice structure. Their values are not independent, but are related by a consistency equation, i.e.,

$$x_A + x_M = 1. \quad (9)$$

By combining (7) with (8) and (9), the strain and the stress of the material can be expressed as a function of the martensitic phase fraction only, as follows

$$\varepsilon = \varepsilon(x_M) = \frac{(E_\pi \varepsilon_T + E_f E_x) x_M + E_f E_M}{kl_0 E_x x_M + E_\pi + kl_0 E_M}, \quad (10)$$

$$\sigma = \sigma(x_M) = E_A E_M \frac{E_f - \varepsilon_T kl_0 x_M}{kl_0 E_x x_M + E_\pi + kl_0 E_M}, \quad (11)$$

where

$$E_\pi = E_A E_M \pi r_0^2, \quad (12)$$

$$E_x = E_A - E_M, \quad (13)$$

$$E_f = k(d - l_0 - y_i). \quad (14)$$

Next, we need to describe the dynamic evolution of the phase fraction. By exploiting concepts from statistical thermodynamics, the following equation is derived

$$\dot{x}_M = -p_{MA} x_M + p_{AM} x_A, \quad (15)$$

where  $p_{AM}$  and  $p_{MA}$  represents the probabilities that a mesoscopic layer of austenite transforms into martensite and vice versa, respectively. The introduction of a similar differential equation for  $x_A$  is not necessary, due to the constraint imposed by (9). The generic transition probability  $p_{\alpha\beta}$  from phase  $\alpha$  to phase  $\beta$  is computed as follows

$$p_{\alpha\beta} = p_{\alpha\beta}(\sigma, T) = \omega_x e^{-\frac{V_L}{k_B T} \Delta g_{\alpha\beta}(\sigma, T)}, \quad (16)$$

where  $\omega_x$  is the vibration frequency associated to the thermal activation,  $V_L$  is the volume of a mesoscopic layer of material,  $k_B$  is the Boltzmann constant,  $T$  is the SMA temperature, and  $\Delta g_{\alpha\beta}(\sigma, T)$  is the stress- and temperature-dependent energy barrier of the phase transformation computed in the Gibbs free-energy density landscape. The energy barriers depend in a complex mathematical way on the transformation stresses of austenite and martensite, denoted as  $\sigma_A$  and  $\sigma_M$  respectively. The explicit dependency is omitted for conciseness (please refer to Seelecke and Müller (2004) for details). For the single-crystal MAS model,  $\sigma_A$  and  $\sigma_M$  are linear functions of  $T$ , i.e.,

$$\sigma_A = \sigma_A(T) = \sigma_A(T_0) + \sigma_T(T - T_0), \quad (17)$$

$$\sigma_M = \sigma_M(T) = \sigma_M(T_0) + \sigma_T(T - T_0), \quad (18)$$

where  $T_0$  is a reference temperature and  $\sigma_T$  is a scaling coefficient.

Finally, the temperature evolution of the SMA can be described via the following internal energy balance equation

$$V \rho_m c_V \dot{T} = -\lambda A_s (T - T_E) + J + V \rho_m H_M \dot{x}_M. \quad (19)$$

In (19),  $V$  is the volume of the SMA wire,  $\rho_m$  is the SMA volumetric mass density,  $c_V$  is the SMA specific heat,  $\lambda$  is the convective cooling coefficient between SMA wire and environment,  $A_s$  is the lateral surface area of the wire,  $T_E$  is the environmental temperature,  $J$  is the input Joule heating, and  $H_M$  is the specific latent heat of the phase transformation.

The complete state model of the SMA-spring actuator can be obtained by collecting equations (10), (15), and (19) in

$$\begin{cases} \dot{x}_M = -p_{MA} x_M + p_{AM} (1 - x_M) \\ \dot{T} = -\frac{\lambda A_s (T - T_E)}{V \rho_m c_V} + \frac{J}{V \rho_m c_V} + \frac{H_M}{c_V} \dot{x}_M \\ \varepsilon = \frac{(E_\pi \varepsilon_T + E_f E_x) x_M + E_f E_M}{kl_0 E_x x_M + E_\pi + kl_0 E_M} \end{cases}. \quad (20)$$

Note that model (20) has two continuous state variables, i.e., the martensitic phase fraction  $x_M$  and the temperature  $T$ . Quantity  $J$  is used as control input,  $T_E$  represents an exogenous disturbance affecting the system, and the SMA strain  $\varepsilon$  describes the actuator output.

Before continuing, the following assumption is considered.

*Assumption 1.* External inputs  $J(t)$  and  $T_E(t)$ , as well as initial conditions  $x_M(0)$  and  $T(0)$ , are such that  $x_M(0) \in [0, 1]$  and  $\varepsilon(t) \geq 0$ ,  $\sigma(t) \geq 0$ ,  $T(t) > 0$ ,  $\forall t \geq 0$ .

Assumption 1 always holds for physically consistent loading conditions and well-designed SMA-spring actuator. In particular, being shaped as a wire, the SMA cannot sustain a compressive stress, and thus  $\varepsilon$  is always non-negative. Consequently, the total forces applied on the moving end of the SMA wire ( $F_{Spring}$ ) must necessarily be greater than (or at least equal to) zero to keep the wire in tension.

### 3. HYBRID DYNAMICAL MODEL

In this section, we propose a hybrid reformulation of model (20) in the framework of Goebel et al. (2012).

#### 3.1 SMA stress approximation

The SMA model in (20) provides a tight description of the response of single-crystal SMA wire spring actuators subject to a number of external inputs. Such a model, however, turns out to be highly involved in terms of computational complexity. The main reason for this issue is due to the transition probabilities appearing in the state equation of  $x_M$ , i.e.,  $p_{MA}$  and  $p_{AM}$ . These quantities are complex to compute since they depend on energy barriers appearing in a non-convex Gibbs free-energy landscape, and have to be evaluated at each step of the numerical ODE integration. In addition, they turn out to be almost discontinuous functions of  $\sigma$  and  $T$ , thus making the resulting model numerically stiff. A potential way to improve the numerical properties of the model, making it more suitable for fast simulations and real-time control applications, would consist in eliminating the stiff dynamics by means of a proper hybrid reformulation of the constitutive equations. The condition that allows us to model the SMA actuator in a hybrid fashion is defined by the following assumption, which is motivated by our earlier results in Rizzello et al. (2018) and Rizzello et al. (2019).

*Assumption 2.* During phase transformation (i.e.,  $\dot{x}_M \neq 0$ ), the SMA stress can be approximated as follows

$$\begin{cases} \sigma(x_M) = \sigma_A(T) & \text{if } \dot{x}_M > 0 \\ \sigma(x_M) = \sigma_M(T) & \text{if } \dot{x}_M < 0 \end{cases}, \quad (21)$$

for  $\sigma(x_M)$ ,  $\sigma_A(T)$ , and  $\sigma_M(T)$  given by (11), (17), and (18), respectively.

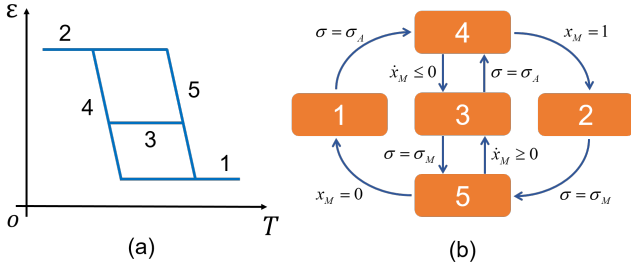


Fig. 3. Example of temperature-strain hysteresis in single-crystal SMA actuator (a) and the graph representation of hybrid automaton with *modes* and *edges* (b).

Assumption 2 holds true with good accuracy for sufficiently large values of  $V_L$  and  $\omega_x$ . This is particularly true for typical values of such physical parameters. For additional considerations on Assumption 2, please refer to the proofs presented in Rizzello et al. (2018) and Rizzello et al. (2019). The above condition will be instrumental for the hybrid reformulation presented in the next section.

### 3.2 SMA hybrid dynamical model

For model (20) it can be observed that, while the Joule heating-strain (i.e., input-output) hysteresis is highly rate-dependent, the shape of the temperature-strain (i.e., second state-output) hysteresis is not affected by the frequency of input signals. A qualitative sketch of such a temperature-strain hysteresis is depicted in Fig. 3(a). This fact allows us to identify five different possible operating modes, also reported in Fig. 3(a), which have the following physical interpretation:

- (1) full austenitic phase  $(x_M = 0)$
- (2) full martensitic phase  $(x_M = 1)$
- (3) inner hysteresis loop  $(x_M = \text{const.}, x_M \in (0, 1))$
- (4) austenite to martensite transformation  $(\dot{x}_M > 0)$
- (5) martensite to austenite transformation  $(\dot{x}_M < 0)$

Regarding the system motion, a hypothetical operating sequence of the model could be the following. The SMA wire starts in a condition of full martensitic crystal lattice (mode 2). When heated by an electric current, the temperature increases to produce a phase change (mode 5). If the input is deactivated before reaching such temperature to obtain the full austenitic phase, the system begins to cool down following an inner hysteresis loop (mode 3), and then it expands (mode 4) up to the initial strain (mode 2). Otherwise, if the wire is heated until it is completely transformed, the maximum contraction of the actuator is obtained (mode 1). The transition between those modes can be described via the hybrid automaton shown in Fig. 3(b), with the set of *modes*  $Q = \{1, 2, 3, 4, 5\}$  and the set of *edges*  $E = \{(1, 4), (4, 2), (2, 5), (5, 1), (4, 3), (3, 5), (5, 3), (3, 4)\}$ . The physical conditions associated to the mode transitions are also reported in Fig. 3(b) (Rizzello et al. (2018)).

By exploiting the above property, we aim at obtaining a reduced-order model in which only the SMA temperature  $T$  appears as a continuous state, while the phase fraction  $x_M$  is expressed as a function of  $T$ . Clearly, different expressions for  $\dot{T}$  and  $x_M$  must be obtained for each mode. In the following, we will use  $\dot{T}^{(i)}$  and  $x_M^{(i)}$  to denote the

derivative of temperature and the phase fraction of the generic mode  $i$ , respectively. Note that, once the phase fraction is known, the system output  $\varepsilon$  can be computed via equation (10) since it is valid for every mode.

*Modes 1,2,3.* The first three modes are characterized by a constant  $x_M^{(i)}$ ,  $i = 1, 2, 3$ , and thus we have  $\dot{x}_M^{(i)} = 0$ . This allows us to simplify the equation (19) as follows

$$\dot{T}^{(i)} = \Phi^{(i)} = \Lambda, \quad i = 1, 2, 3, \quad (22)$$

where  $\Phi^{(i)}$  is an auxiliary function, and

$$\Lambda = \Lambda(T, T_E, J) = \frac{J - \lambda A_s (T - T_E)}{V \rho_m c_V}. \quad (23)$$

Concerning the constant value of  $x_M^{(i)}$ , we have that  $x_M^{(1)} = 0$ ,  $x_M^{(2)} = 1$ , while  $x_M^{(3)}$  coincides with the value that such variable had prior to the jump to mode 3.

*Mode 4.* In mode 4 the phase fraction increases over time, i.e.,  $\dot{x}_M > 0$ . In this case, we can replace (11) and (17) in (21), and solve the resulting equation for  $x_M^{(4)}$ . In this way,  $x_M^{(4)}$  can be expressed as a function of  $T$  as follows

$$x_M^{(4)} = x_M^{(4)}(T) = \frac{1}{kl_0} \frac{-(E_\pi + E_M kl_0) \sigma_A(T) + E_A E_f}{E_x \sigma_A(T) + E_A E_M \varepsilon_T}. \quad (24)$$

By differentiating (24) over time and replacing it in (19), we obtain

$$\dot{T}^{(4)} = \Phi^{(4)} = \Lambda + \frac{H_M}{c_V} \underbrace{\frac{-E_A E_M c_V M \Lambda}{c_V l_0 k \Sigma_A^2 + E_A E_M H_M M}}_{\dot{x}_M^{(4)}}, \quad (25)$$

where

$$M = (E_x E_f + \varepsilon_T (E_\pi + E_M kl_0)) \sigma_T, \quad (26)$$

$$\Sigma_A = \Sigma_A(T) = E_x \sigma_A(T) + E_A E_M \varepsilon_T. \quad (27)$$

Lastly, we define a new function

$$s_M^{(4)} = s_M^{(4)}(T) = -\frac{E_A E_M c_V M \Lambda}{c_V l_0 k \Sigma_A^2 + E_A E_M H_M M}, \quad (28)$$

that physically corresponds to  $\dot{x}_M^{(4)}$ .

*Mode 5.* In mode 5,  $\dot{x}_M < 0$  always holds. The procedure used for mode 4 can be applied also here in a straightforward way, provided that we replace  $\sigma_A(T)$  with  $\sigma_M(T)$  in (24)-(27). The resulting equations for  $x_M^{(5)}$  and  $\dot{T}^{(5)}$  are reported in the following

$$x_M^{(5)} = x_M(T) = \frac{1}{kl_0} \frac{-(E_\pi + E_M kl_0) \sigma_M(T) + E_A E_f}{E_x \sigma_M(T) + E_A E_M \varepsilon_T}, \quad (29)$$

$$\dot{T}^{(5)} = \Phi^{(5)} = \Lambda + \frac{H_M}{c_V} \underbrace{\frac{-E_A E_M c_V M \Lambda}{c_V l_0 k \Sigma_M^2 + E_A E_M H_M M}}_{\dot{x}_M^{(5)}}, \quad (30)$$

where  $M$  is as in (26), and

$$\Sigma_M = \Sigma_M(T) = E_x \sigma_M(T) + E_A E_M \varepsilon_T. \quad (31)$$

As for the previous mode, we can define a new function

$$s_M^{(5)} = s_M^{(5)}(T) = -\frac{E_A E_M c_V M \Lambda}{c_V l_0 k \Sigma_M^2 + E_A E_M H_M M}, \quad (32)$$

that physically corresponds to  $\dot{x}_M^{(5)}$ .

Now we are in a position to reformulate the considered actuator as a hybrid dynamical system with state  $x :=$

$(x_1, x_2, q) = (T, x_d, q) \in (\mathbb{R}_{\geq 0} \times [0, 1] \times \{1, 2, 3, 4, 5\})$ , where  $T$  is the temperature,  $x_d$  is the *discrete phase fraction*, i.e., the value of the phase fraction  $x_M$  at the time of the previous mode change, and  $q$  is a numerical index characterizing the active mode.

Based on these facts, we define the *flow set* as

$$C := \bigcup_{i=1}^5 C_i, \quad (33)$$

where

$$C_1 := (\{x_1 \in \mathbb{R}_{\geq 0} : x_M^{(4)}(x_1) \leq 0\} \times \{0\} \times \{1\}), \quad (34)$$

$$C_2 := (\{x_1 \in \mathbb{R}_{\geq 0} : x_M^{(5)}(x_1) \geq 1\} \times \{1\} \times \{2\}), \quad (35)$$

$$C_3 := (\{x_1 \in \mathbb{R}_{\geq 0} : \sigma_M(x_1) \leq \sigma(x_2) \leq \sigma_A(x_1)\} \times [0, 1] \times \{3\}), \quad (36)$$

$$C_4 := (\{x_1 \in \mathbb{R}_{\geq 0} : x_M^{(4)}(x_1) \leq 1, s_M^{(4)}(x_1) \geq 0\} \times [0, 1] \times \{4\}), \quad (37)$$

$$C_5 := (\{x_1 \in \mathbb{R}_{\geq 0} : x_M^{(5)}(x_1) \geq 0, s_M^{(5)}(x_1) \leq 0\} \times [0, 1] \times \{5\}), \quad (38)$$

and, for all  $x \in C$ , the *flow map* as

$$f(x) := (\Phi^{(q)}(x_1), 0, 0) \quad (39)$$

where  $\Phi^{(q)}(x_1)$  for all  $q \in \{1, 2, 3, 4, 5\}$  are defined in (22), (25), and (30). States  $x_2$  and  $q$  are constant during flows and change only at jumps. To capture the instantaneous changes undergone by the system state, we define the *jump set* as

$$D := \bigcup_{i=1}^8 D_i, \quad (40)$$

where

$$D_1 := (\{x_1 \in \mathbb{R}_{\geq 0} : x_M^{(4)}(x_1) \geq 0\} \times \{0\} \times \{1\}), \quad (41)$$

$$D_2 := (\{x_1 \in \mathbb{R}_{\geq 0} : x_M^{(5)}(x_1) \leq 1\} \times \{1\} \times \{2\}), \quad (42)$$

$$D_3 := (\{x_1 \in \mathbb{R}_{\geq 0} : \sigma_M(x_1) \geq \sigma(x_2)\} \times [0, 1] \times \{3\}), \quad (43)$$

$$D_4 := (\{x_1 \in \mathbb{R}_{\geq 0} : \sigma(x_2) \geq \sigma_A(x_1)\} \times [0, 1] \times \{3\}), \quad (44)$$

$$D_5 := (\{x_1 \in \mathbb{R}_{\geq 0} : x_M^{(4)}(x_1) \geq 1\} \times [0, 1] \times \{4\}), \quad (45)$$

$$D_6 := (\{x_1 \in \mathbb{R}_{\geq 0} : s_M^{(4)}(x_1) \leq 0\} \times [0, 1] \times \{4\}), \quad (46)$$

$$D_7 := (\{x_1 \in \mathbb{R}_{\geq 0} : x_M^{(5)}(x_1) \leq 0\} \times [0, 1] \times \{5\}), \quad (47)$$

$$D_8 := (\{x_1 \in \mathbb{R}_{\geq 0} : s_M^{(5)}(x_1) \geq 0\} \times [0, 1] \times \{5\}), \quad (48)$$

and, for all  $x \in D$ , we define the set-valued *jump map* as

$$G(x) := \bigcup_{i \in \{k \in \{1, 2, \dots, 8\} : x \in D_k\}} g_i(x), \quad (49)$$

where

$$g_1(x) := (x_1, 0, 4) \quad \forall x \in D_1 \quad (50)$$

$$g_2(x) := (x_1, 1, 5) \quad \forall x \in D_2 \quad (51)$$

$$g_3(x) := (x_1, x_2, 5) \quad \forall x \in D_3 \quad (52)$$

$$g_4(x) := (x_1, x_2, 4) \quad \forall x \in D_4 \quad (53)$$

$$g_5(x) := (x_1, 1, 2) \quad \forall x \in D_5 \quad (54)$$

$$g_6(x) := (x_1, x_M^{(4)}(x_1), 3) \quad \forall x \in D_6 \quad (55)$$

$$g_7(x) := (x_1, 0, 1) \quad \forall x \in D_7 \quad (56)$$

$$g_8(x) := (x_1, x_M^{(5)}(x_1), 3) \quad \forall x \in D_8 \quad (57)$$

Therefore, the considered actuator can be modeled via the hybrid system  $\mathcal{H} = (C, f, D, G)$ .

*Remark 1.* It can be noticed that hybrid system  $\mathcal{H}$  satisfies the so-called hybrid basic conditions; see (Goebel et al., 2012, Assumption 6.5, page 120). As such, the proposed model has some interesting robustness properties with respect to small perturbations. This feature, among other things, makes it this model highly suitable for numerical simulations.

#### 4. SIMULATION AND RESULTS

To simulate the hybrid system  $\mathcal{H}$  in Matlab environment, we use the *Hybrid Equation (HyEQ) Toolbox*, described in Sanfelice et al. (2013). In this case, the hybrid model of the SMA actuator is implemented using the *Lite HyEQ Simulator*, available inside the toolbox. Numerical integration is carried out via *ode45* solver. For comparison purpose, the physics-based model described by (20) is implemented in Matlab as a standard ODE model. Due to the high numerical stiffness of such a model, *ode15s* is chosen as a solver. All simulations are conducted by considering an actuator with  $d = 0.1$  m, a spring with an initial length  $y_i = 0.0445$  m and constant  $k = 1000$  N/m, coupled with a  $l_0 = 0.05$  m SMA wire long. The other SMA physical parameters are chosen as in Rizzello et al. (2019).

A comparative simulation study between the two models is reported in Fig. (4). The figure shows the wire response when subject to a time-varying Joule heating, chosen in such a way that all modes are explored, and a constant environmental temperature  $T_E = 293$  K. Results of hybrid and MAS models are shown as solid blue lines and dashed red lines, respectively. For the hybrid model only, the jumps are marked with solid dots. Results are presented in terms of input Joule heating (top-left), resulting temperature (top-right), output strain (bottom-left), and modes jumps (bottom-right, for hybrid model only).

It can be seen that the results of both models are practically overlapped (with a peak error lower than the tolerance of the numerical solver), thus making the hybrid reformulation highly accurate. In addition, it can be observed how the hybrid model can be integrated in a significantly smaller time compared to the previous model. Using non-canonical input signals, i.e., random sequences of variable amplitude steps, the simulation time of the hybrid model is up to 100 times smaller than the previous model (0.22 s vs. 23.43 s required to simulate 20 s of the actuator response).

For concluding this section, Fig. (5) shows the Joule heating-strain (left-hand side) and temperature-strain (right-hand side) trajectories, for the same simulation described above. Due to the high accuracy observed in Fig. (4), only the results of the hybrid model are shown. From Fig. (5), the hysteretic behavior of the actuator can readily be observed. In addition, it can be seen that while the temperature-strain hysteresis has a piecewise linear shape, the Joule heating-strain hysteresis is more smooth. This is due to the SMA thermal dynamics, which results into a rate-dependent input-output hysteresis. By means of the developed hybrid model, accurate description of this rate-dependent hysteresis can be achieved in a physics-based and numerically efficient fashion.

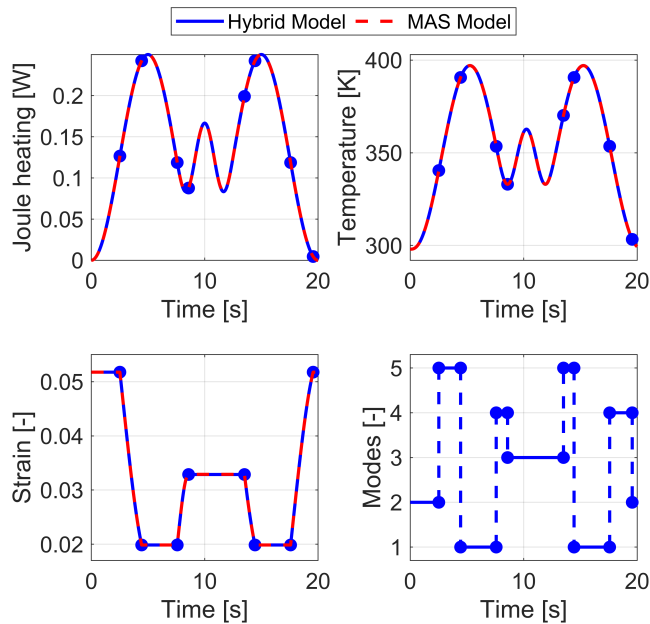


Fig. 4. Comparison between the hybrid dynamical model (solid blue line) and MAS model (dashed red line).

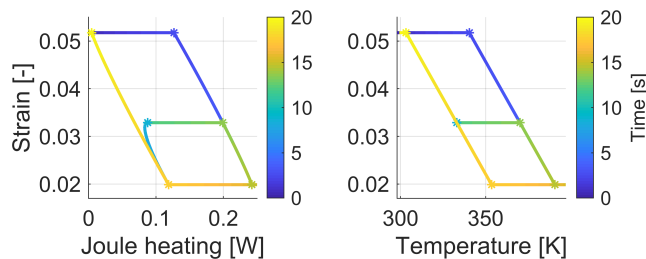


Fig. 5. Characteristic curves of the SMA-spring actuator: input-output hysteresis (left-hand side) and state-output hysteresis (right-hand side).

## 5. CONCLUSIONS

In this paper, a hybrid hysteresis model has been presented for a single-crystal SMA wire actuator coupled with a bias spring. The obtained model is based on a hybrid reformulation of the physics-based model for SMA wires developed by Müller-Achenbach-Seelecke. It has been shown how, through a proper reasoning on the SMA constitutive equations, it is possible to reformulate the physics-based model as a reduced order hybrid dynamical system which combines continuous-time and discrete-time dynamics. Compared to the physics-based model, the hybrid one permits to achieve the same accuracy with a significantly lower computational time. At the same time, differently from alternative hysteresis model commonly used in control applications (e.g., Preisach), it accounts for the effects of physical parameters such as loading forces, environmental temperatures, and wire geometry, thus it can be also used for fast model-based actuator optimization. In future studies, a more generic SMA hybrid model will be presented to account for the more complex behavior of polycrystalline wires, i.e., SMAs which exhibit a smooth hysteresis with minor loops. The developed model will then open up the possibility to apply hybrid control theory on SMA devices.

## REFERENCES

- Cianchetti, M., Licofonte, A., Follador, M., Rogai, F., and Laschi, C. (2014). Bioinspired soft actuation system using shape memory alloys. *Actuators*, 3, 226–244.
- Goebel, R., Sanfelice, R.G., and Teel, A.R. (2012). *Hybrid Dynamical Systems: Modeling, Stability, and Robustness*. Princeton University Press, New Jersey.
- Janaideh, M., Naldi, R., Marconi, L., and Krejci, P. (2012). A hybrid system for a class of hysteresis nonlinearity: Modeling and compensation. *IEEE Conference on Decision and Control (CDC)*, 5380–5385.
- Lagoudas, D. (2008). *Shape Memory Alloys: Modeling and Engineering Applications*. Springer ebook collection / Chemistry and Materials Science 2005-2008. Springer US.
- Ramirez-Laboreo, E., Roes, M., and Sagues, C. (2019). Hybrid dynamical model for reluctance actuators including saturation, hysteresis and eddy currents. *IEEE/ASME Transactions on Mechatronics*, 24, 1396–1406.
- Rizzello, G., Naso, D., and Seelecke, S. (2018). Passivity analysis and port-hamiltonian formulation of the Müller-Achenbach-Seelecke model for shape memory alloys: the isothermal case. *IFAC-PapersOnLine*, 51, 713–718.
- Rizzello, G., Naso, D., and Seelecke, S. (2019). Hysteresis modeling in thermal shape memory alloy wire actuators: an irreversible port-hamiltonian approach. *2019 IEEE 58th Conference on Decision and Control (CDC)*, 7937–7943.
- Sanfelice, R.G., Copp, D.A., and Nanez, P. (2013). A toolbox for simulation of hybrid systems in Matlab/Simulink: Hybrid Equations (HyEQ) Toolbox. In *Proceedings of Hybrid Systems: Computation and Control Conference*, 101–106.
- Seelecke, S. and Müller, I. (2004). Shape memory alloy actuators in smart structures: Modeling and simulation. *Applied Mechanics Reviews - APPL MECH REV*, 57, 23.
- Shakiba, S., Yousefi-Koma, A., Jokar, M., Zakerzadeh, M.R., and Basaeri, H. (2019). Modeling and characterization of the shape memory alloybased morphing wing behavior using proposed rate-dependent prandtl-ishlinskii models. *Proceedings of the Institution of Mechanical Engineers, Part I: Journal of Systems and Control Engineering*, 1–16.
- Shao, S., Xu, M., Zhang, S., and Xie, S. (2016). Stroke maximizing and high efficient hysteresis hybrid modeling for a rhombic piezoelectric actuator. *Mechanical Systems and Signal Processing*, 75, 631 – 647.
- Tiboni, M., Borboni, A., Mor, M., and Pomi, D. (2011). An innovative pneumatic mini-valve actuated by sma ni-ti wires: design and analysis. *Proceedings of the Institution of Mechanical Engineers, Part I: Journal of Systems and Control Engineering*, 225(3), 443–451.
- Toledo, L.F., Ge, J.Z., Oxoby, J.M., Chen, Y., and Prez-Arancibia, N.O. (2017). System identification of a niti-based sma actuator using a modified preisach model and adaptive control. *2017 American Control Conference (ACC)*, 183–190.